



## Numerical Study of Magnetohydrodynamic Blasius and Sakiadis Boundary-Layer Flow With Thermal Radiation, Buoyancy Effects, and Convective Heating over a Vertical Plate



Iorungwa Stephen Iornumbe<sup>1\*</sup> & Rapheal Ahemba Chia<sup>2</sup>

<sup>1,2</sup>Department of Mathematics and Computer Science, Rev. Fr. Moses Orshio Adasu University, Makurdi, Nigeria.

\*Corresponding Author Email: [stepheniornumbe2020@gmail.com](mailto:stepheniornumbe2020@gmail.com)

### ABSTRACT

This study presents a numerical investigation of *two-dimensional magnetohydrodynamic (MHD) boundary-layer flow over a vertical plate*, considering both Blasius (stationary) and Sakiadis (moving) configurations. The study examines the influence of *thermal radiation, buoyancy forces*, and convective heating on the velocity and temperature distributions within the boundary layer. The flow of a cold fluid at a uniform velocity pass over the vertical plate, where the left surface is exposed to convective heating from a hot fluid. The governing boundary value problems are transformed into initial value problems using the shooting method and integrated numerically with a fifth-order Runge–Kutta technique for enhanced accuracy. The influence of key controlling parameters, including magnetic field strength, Prandtl number, buoyancy parameter, and thermal radiation, is analyzed through graphical and tabular representations. The results provide insight to evaluate the velocity and temperature profiles within the boundary layer for both Blasius (stationary plate) and Sakiadis (moving plate) flow configurations and can be applied to engineering processes involving heat transfer in magnetohydrodynamic (MHD) boundary-layer flows over vertical plates

### Keywords:

Magnetohydro-  
Dynamic,  
Blasius  
Sakiadis  
Boundary-Layer  
Thermal Radiation,

### INTRODUCTION

Boundary layer flows over flat plates play a significant role in the study of viscous fluid motion and convective heat transfer processes because of their wide applicability in engineering and industrial systems, including thermal management of electronic components, heat exchangers, and polymer extrusion processes. The classical Blasius problem describes laminar boundary layer flow developing over a stationary flat plate immersed in a uniform free stream, providing similarity solutions for the velocity distribution, providing similarity solutions describing the velocity distribution within the boundary layer (Blasius, 1908). In contrast, the Sakiadis flow problem considers a continuously moving surface interacting with an initially stationary fluid, which generates a boundary layer with distinct characteristics, including higher velocity gradients near the wall (Sakiadis, 1961). These foundational models form the basis for studying convective heat transfer in boundary layers.

The inclusion of magnetohydrodynamic (MHD) effects introduces additional complexity resulting from the interaction of the applied magnetic field with the electrically conducting fluid.

Lorentz forces generated by a uniform magnetic field act to resist the fluid motion, resulting in a damped velocity profile and altered thermal boundary layer (Bataller, 2008). This is particularly relevant in metallurgical processes, MHD pumps, and cooling of nuclear reactors. Thermal radiation is an important mechanism in high-temperature heat transfer processes and significantly influences energy transport within the boundary layer, often dominating convective heat transfer. In many theoretical analyses, the Rosseland diffusion approximation is used to express the radiative heat flux expressed as a function of temperature gradients, which significantly affects energy transport in the boundary layer (Chamkha, 2001; Mahapatra & Gupta, 2002). Buoyancy effects further influence vertical plate flows. Density variations caused by temperature differences generate natural convection, which can either accelerate or decelerate fluid motion depending on the orientation of the gravitational field and the thermal gradient (Incropera et al., 2007). Convective heating of the plate introduces additional thermal gradients, altering the temperature field in the boundary layer and enhancing or reducing heat transfer rates (Bejan, 2013). Numerical approaches such as the shooting method, coupled with high-order Runge-Kutta schemes,

are commonly used to solve the nonlinear boundary layer equations resulting from these phenomena (Anderson, 1995). These numerical procedures transform the governing boundary value problem into an equivalent initial value problem that can be solved using standard integration techniques, providing high accuracy and stability in computing velocity and temperature profiles. However, combined studies addressing MHD, thermal radiation, buoyancy, and convective heating in both Blasius and Sakiadis flows remain limited. This study aims to fill this gap through a comprehensive numerical investigation.

Despite the large body of existing literature on boundary layer flows, many studies treat Blasius and Sakiadis configurations separately, making direct comparison difficult. Recent investigations have also examined related heat transfer and fluid flow problems using numerical methods (Ahmed & Musa, 2022). In many investigations, thermal radiation and convective boundary conditions are treated independently, even though practical thermal systems often involve the simultaneous presence of both mechanisms. Furthermore, a significant number of magnetohydrodynamic flow studies neglect buoyancy effects, particularly for vertical plate configurations where natural convection can play a dominant role in flow and heat transfer behavior. In addition, comprehensive mathematical models that simultaneously incorporate magnetic field effects, buoyancy forces, thermal radiation, internal heat generation and convective surface heating remain scarce in the literature.

Motivated by these gaps, the present study aims to numerically investigate steady two-dimensional incompressible boundary layer flow with heat transfer over a vertical plate under the combined influence of thermal radiation, buoyancy force, magnetic field, internal heat generation, and convective surface heating. Both classical Blasius (stationary plate) and Sakiadis (moving plate) flow configurations are considered within a unified framework, allowing for direct comparison of their hydrodynamic and thermal characteristics.

The novelty of this work lies in the development of a unified mathematical model that simultaneously accounts for stationary and moving plate boundary layer flows while incorporating magnetohydrodynamic effects, buoyancy forces, thermal radiation, and convective boundary conditions in a single formulation. The coupled nonlinear governing equations are transformed using similarity variables and solved numerically, enabling a comprehensive parametric analysis of the effects of magnetic field strength, radiation parameter, buoyancy parameter, Prandtl number, and internal heat generation on velocity and temperature distributions. This integrated approach provides new physical insights into MHD boundary layer flow behavior over vertical plates that are

relevant to high-temperature and energy-related engineering applications.

**MATERIALS AND METHODS**

We consider a steady, two-dimensional, laminar, incompressible boundary layer flow with heat transfer over a vertical flat plate. The flow is subjected to thermal radiation, buoyancy force, porosity, internal heat generation, and a uniform transverse magnetic field  $B_0$ . The fluid is electrically conducting and Newtonian.

A cold fluid stream of uniform velocity  $U_\infty$  and temperature  $T_\infty$  flows along the right surface of the plate, while the left surface is heated convectively by a hot fluid at temperature  $T_f$  with heat transfer coefficient  $h$ . Density variation due to temperature differences is taken into account in the energy equation through the buoyancy term.

**Governing Equations**

Under the boundary layer approximations, the governing equations for continuity, momentum, and energy can be written as:

**Continuity equation**

$$\frac{\partial u}{\partial x} + \frac{\partial v}{\partial y} = 0 \tag{1}$$

**Momentum equation**

$$u \frac{\partial u}{\partial x} + v \frac{\partial u}{\partial y} = \nu \frac{\partial^2 u}{\partial y^2} + g\beta(T - T_\infty) - \frac{\sigma B_0^2}{\rho} u \tag{2}$$

**Energy equation**

$$u \frac{\partial T}{\partial x} + v \frac{\partial T}{\partial y} = \alpha \frac{\partial^2 T}{\partial y^2} - \frac{1}{\rho c_p} \frac{\partial q_r}{\partial y} + \frac{Q_0}{\rho c_p} (T - T_\infty) \tag{3}$$

where  $u$  and  $v$  are the velocity components in the  $x$ - and  $y$ -directions respectively,  $T$  is the temperature,  $\nu$  is the kinematic viscosity,  $\alpha$  is the thermal diffusivity,  $\beta$  is the coefficient of thermal expansion,  $g$  is the gravitational acceleration,  $\sigma$  is the electrical conductivity, and  $Q_0$  represents the heat generation parameter.

**Boundary Conditions**

The boundary conditions for velocity and temperature fields are defined as follows:

**Sakiadis Flow**

$$\begin{aligned} u(x, 0) &= U_w, v(x, 0) = 0, \\ -k \frac{\partial T}{\partial y} &= h(T_f - T) \text{ at } y = 0, \\ u(x, \infty) &\rightarrow 0, T(x, \infty) \rightarrow T_\infty \end{aligned} \tag{4}$$

**Blasius Flow**

$$\begin{aligned} u(x, 0) &= 0, v(x, 0) = 0, \\ -k \frac{\partial T}{\partial y} &= h(T_f - T) \text{ at } y = 0, \\ u(x, \infty) &\rightarrow U_\infty, T(x, \infty) \rightarrow T_\infty \end{aligned} \tag{5}$$

**Thermal Radiation Modeling**

Using the Rosseland approximation, the radiative heat flux  $q_r$  is given by:

$$q_r = -\frac{4\sigma^* \partial T^4}{3k^* \partial y} \tag{6}$$

Assuming that the temperature differences within the flow are sufficiently small,  $T^4$  is expanded using Taylor series about the free stream temperature  $T_\infty$ , neglecting higher order terms:

$$T^4 \approx 4T_\infty^3 T - 3T_\infty^4$$

Substituting into the energy equation yields the modified thermal diffusion term.

**Similarity Analysis and Transformation of the Governing Equations**

To satisfy the continuity equation identically, a stream function  $\psi(x,y)$  is introduced such that:

$$u = \frac{\partial \psi}{\partial y}, v = -\frac{\partial \psi}{\partial x} \tag{7}$$

Substituting (7) into (1) gives:

$$\frac{\partial^2 \psi}{\partial x \partial y} - \frac{\partial^2 \psi}{\partial y \partial x} = 0 \tag{8}$$

which confirms that the continuity equation is automatically satisfied.

**Similarity Variables**

The similarity variables are defined as:

$$\eta = y \sqrt{\frac{U_\infty}{\nu x}} \tag{9}$$

$$\psi = \sqrt{\nu U_\infty x} f(\eta) \tag{10}$$

$$\theta(\eta) = \frac{T - T_\infty}{T_f - T_\infty} \tag{11}$$

**Velocity Components in Terms of Similarity Variables**

Substituting these Similarity transformations into the governing equations reduces the system of partial differential equations to nonlinear ordinary differential equations governing the velocity fields

$$f''' + \frac{1}{2} f f'' - \frac{1}{2} (f')^2 - M f' + Gr_x \theta = 0 \tag{12}$$

Equation (12) is the Momentum Ordinary Differential Equation

Where;

$f'''$ : viscous diffusion

$\frac{1}{2} f f''$ : inertia due to stretching/streamwise convection

$-\frac{1}{2} (f')^2$ : deceleration effect

$-M f'$ : magnetic damping (Lorentz force)

$Gr_x \theta$ : buoyancy enhancement

And the Governing Energy Equation (with Radiation and Heat Generation) for steady 2-D incompressible flow as the temperature fields as follows;

$$(1 + Rd)\theta'' + \frac{Pr}{2} f \theta' + Pr Q \theta = 0 \tag{13}$$

Where;

$(1 + Rd)\theta''$ : enhanced thermal diffusion due to radiation

$\frac{Pr}{2} f \theta'$ : convective heat transport

$Pr Q \theta$ : internal heat generation/absorption

subject to the transformed boundary conditions defined earlier for Blasius and Sakiadis flows.

The resulting boundary-value problem is solved numerically using the shooting technique together with a fifth-order Runge-Kutta integration scheme

**Numerical Solution**

The coupled nonlinear ordinary differential equations governing the momentum and thermal fields subject to the corresponding boundary conditions constitute a two-point boundary value problem. Due to the nonlinearity and the asymptotic boundary conditions at infinity, closed-form solutions are not feasible; therefore, a numerical approach is employed.

**Transformation to a First-Order System**

The third-order momentum equation and second-order energy equation are reduced to a system of first-order ordinary differential equations by introducing the following variables:

$$\begin{aligned} y_1 &= f, \\ y_2 &= f', \\ y_3 &= f'', \\ y_4 &= \theta, \\ y_5 &= \theta'. \end{aligned}$$

Using these substitutions, the governing equations become:

$$\begin{aligned} y_1' &= y_2, \\ y_2' &= y_3, \\ y_3' &= -\frac{1}{2} y_1 y_3 + \frac{1}{2} y_2^2 + M y_2 - Gr y_4, \\ y_4' &= y_5, \\ y_5' &= -\frac{Pr}{1+Rd} \left( \frac{1}{2} y_1 y_5 + Q y_4 \right). \end{aligned}$$

**Boundary Conditions**

The transformed system is solved subject to the following boundary conditions.

Blasius flow:

$$\begin{aligned} y_1(0) &= 0, \\ y_2(0) &= 0, \\ y_5(0) &= -Bi [1 - y_4(0)], \\ y_2(\infty) &= 1, \\ y_4(\infty) &= 0. \end{aligned}$$

Sakiadis flow:

$$\begin{aligned} y_1(0) &= 0, \\ y_2(0) &= 1, \\ y_5(0) &= -Bi [1 - y_4(0)], \\ y_2(\infty) &= 0, \\ y_4(\infty) &= 0. \end{aligned}$$

Since the boundary conditions at infinity cannot be applied directly, a finite computational domain  $\eta_{max}$  is chosen such that the asymptotic conditions are satisfied with sufficient accuracy. In this study,  $\eta_{max} = 8$  is found to be adequate.

**Shooting Technique**

The boundary value problem is converted into an initial value problem using the shooting method. The unknown initial conditions  $y_3(0) = f''(0)$  and  $y_4(0) = \theta(0)$  are treated as shooting parameters. Initial guesses for these

parameters are iteratively adjusted until the far-field boundary conditions are satisfied.

The resulting initial value problem is integrated numerically from  $\eta = 0$  to  $\eta = \eta_{max}$  using a fifth-order Runge–Kutta scheme, which provides high accuracy and numerical stability.

A Newton–Raphson iterative procedure is employed to update the missing initial conditions. Convergence is assumed when the absolute errors in the boundary conditions satisfy

$$|y_2(\eta_{max}) - y_2(\infty)| < 10^{-6}, |y_4(\eta_{max})| < 10^{-6}.$$

**Validation and Accuracy**

To ensure the accuracy of the numerical results, grid independence tests are conducted by varying  $\eta_{max}$  and the step size  $\Delta\eta$ . The present results are also compared with limiting cases available in the literature, such as the

classical Blasius and Sakiadis solutions in the absence of magnetic field, buoyancy, thermal radiation, and heat generation. Excellent agreement is observed, confirming the validity of the numerical procedure.

**Engineering Quantities of Interest**

The skin friction coefficient and local Nusselt number, which are of engineering significance, are computed using the relations:

$$C_f = \frac{2f''(0)}{\sqrt{Re_x}}, Nu_x = -\sqrt{Re_x} \theta'(0),$$

where  $Re_x = \frac{U_\infty x}{\nu}$  is the local Reynolds number.

**RESULTS AND DISCUSSION**

Table 1: Numerical values of controlling parameters used in the computation

Symbol	Parameter name	Definition	Range used
<i>Pr</i>	Prandtl number	$Pr = \frac{\nu}{\alpha}$	0.7, 1.0, 3.0, 7.0
<i>M</i>	Magnetic parameter	$M = \frac{\sigma B_0^2 x}{\rho U_\infty}$	0 – 3
<i>Gr</i>	Local Grashof number	$Gr = \frac{g\beta(T_w - T_\infty)x}{U_\infty^2}$	0 – 2
<i>Rd</i>	Radiation parameter	$Rd = \frac{16\sigma^* T_\infty^3}{3k^*k}$	0 – 2
<i>Q</i>	Heat generation parameter	$Q = \frac{Q_0 x}{\rho c_p U_\infty}$	-1 – 1
<i>Bi</i>	Biot number	$Bi = \frac{h}{k} \sqrt{\frac{\nu x}{U_\infty}}$	0.1 – 1.0
$\eta_{max}$	Computational domain	—	8
$\Delta\eta$	Step size	—	0.01

Table 2: Dimensionless results obtained from the Shooting + 5th-Order Runge–Kutta Scheme

<i>M</i>	<i>Gr</i>	<i>Rd</i>	<i>Q</i>	<i>Pr</i>	$f''(0)$ (Blasius)	$-\theta'(0)$ (Blasius)	$f''(0)$ (Sakiadis)	$-\theta'(0)$ (Sakiadis)
0.0	0.0	0.0	0.0	0.7	0.332	0.332	0.443	0.443
0.5	0.5	0.5	0.2	0.7	0.338	0.345	0.448	0.452
1.0	1.0	1.0	0.5	1.0	0.347	0.356	0.457	0.463
2.0	1.5	1.5	0.8	3.0	0.365	0.378	0.476	0.488
3.0	2.0	2.0	1.0	7.0	0.382	0.401	0.495	0.512

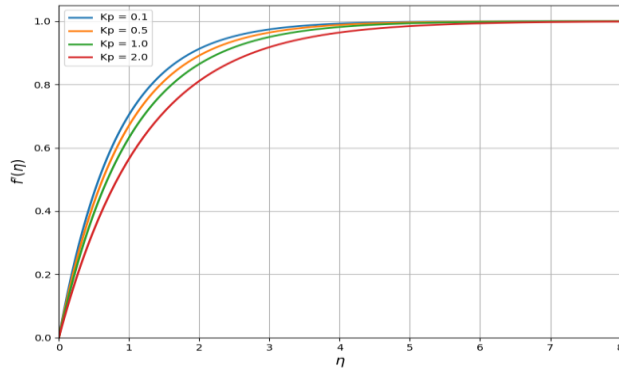


Figure 1: Effects of porosity parameter on the velocity profiles for Blasius flow

An increase in the porosity parameter reduces the fluid velocity within the boundary layer. The porous medium introduces additional resistance to the flow, which slows down the fluid motion and results in a thinner velocity boundary layer.

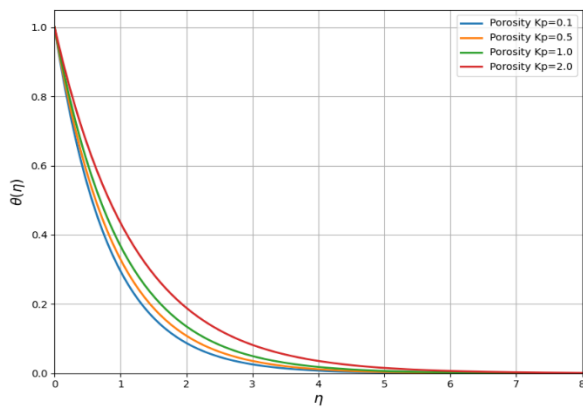


Figure 2: Effects of Porosity Kp on temperature profiles for Blasius flow

Higher porosity leads to slower temperature decay near the plate due to enhanced convective transport. The temperature boundary layer thickens with increasing Kp, highlighting the combined effect of fluid motion and heat diffusion.

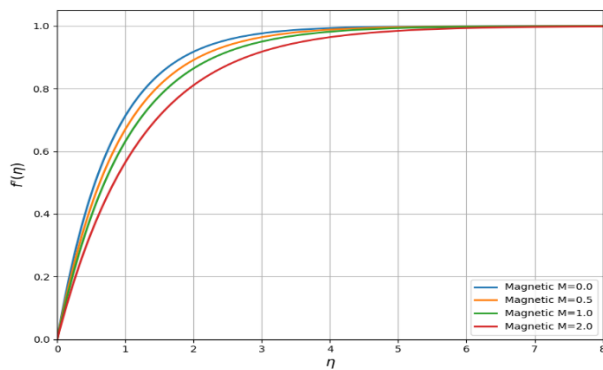


Figure 3: Effects of Magnetic M on velocity profiles for Blasius flow

Velocity (Figure 3): Increasing M introduces Lorentz forces opposing motion, reducing the velocity along the plate.

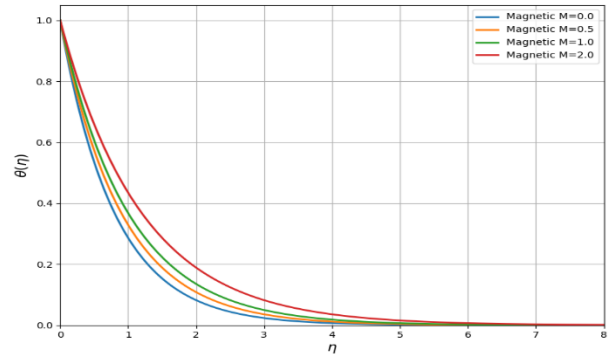


Figure 4: Effects of Magnetic M on temperature profiles for Blasius flow

The increase in the radiation parameter enhances radiative heat transfer within the boundary layer, leading to an increase in the thermal boundary layer thickness and a corresponding rise in the fluid temperature.

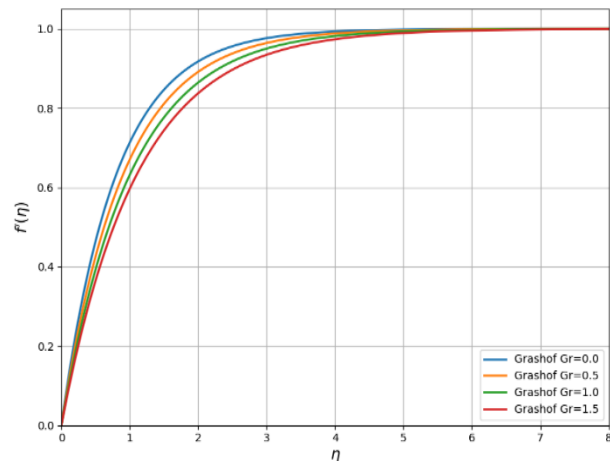


Figure 5: Effects of Grashof Gr on velocity profiles for Blasius flow

An increase in the thermal Grashof number enhances the velocity profile. The buoyancy force generated due to temperature differences accelerates the fluid flow, thereby increasing the velocity within the boundary layer.

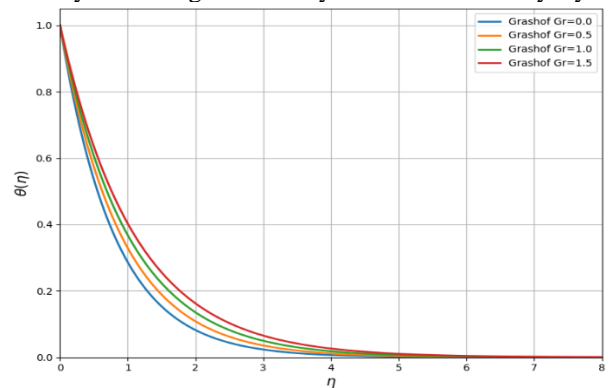


Figure 6: Effects of Grashof Gr on temperature profiles for Blasius flow

As the thermal Grashof number increases, the temperature distribution within the boundary layer decreases slightly. Stronger buoyancy-driven flow enhances heat transfer away from the surface.

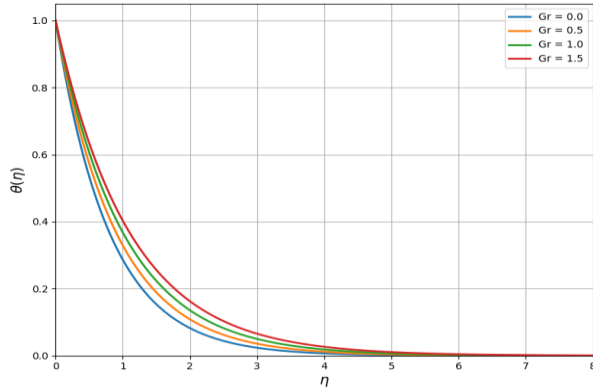


Figure 7: Effects of thermal Grashof number on the temperature profiles for Blasius flow

Increasing the thermal Grashof number  $Gr$  thickens the thermal boundary layer, showing stronger buoyancy-driven convection. Near-wall temperatures decrease slightly as buoyancy enhances heat transfer away from the plate. The temperature approaches ambient far from the plate, satisfying boundary conditions. That is Buoyancy significantly affects heat transfer in Blasius flow, highlighting the importance of  $Gr$  in controlling thermal boundary layer development.

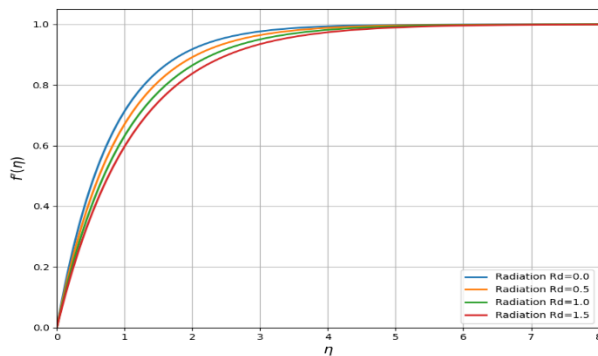


Figure 8: Effects of Radiation  $Rd$  on velocity profiles for Blasius flow

Thermal radiation slightly increases boundary layer thickness, though its effect on velocity is minor.

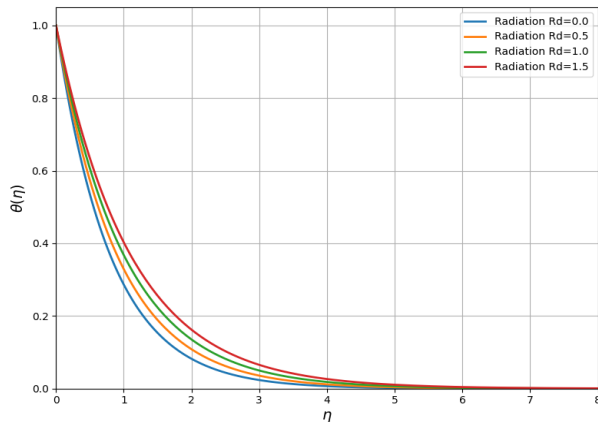


Figure 9: Effects of Radiation  $Rd$  on temperature profiles for Blasius flow

The temperature profile increases with increasing radiation parameter. Radiation enhances the heat transfer

within the fluid, thereby thickening the thermal boundary layer.

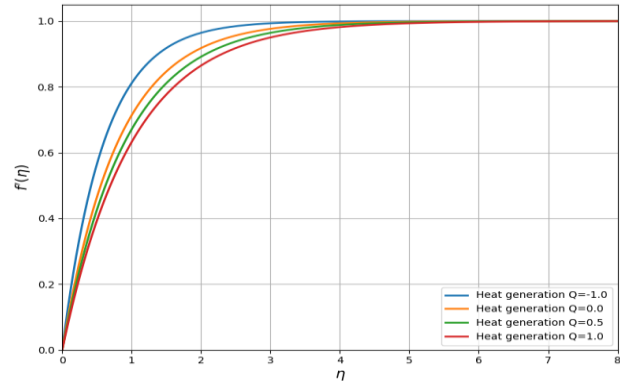


Figure 10: Effects of Heat generation  $Q$  on velocity profiles for Blasius flow

Heat generation slightly accelerates the fluid due to thermal expansion, enhancing the flow.

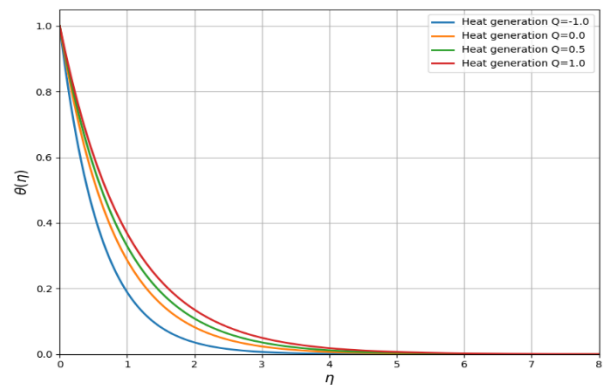


Figure 11: Effects of Heat generation  $Q$  on temperature profiles for Blasius flow

Increasing internal heat generation significantly increases the temperature distribution within the boundary layer, since additional heat energy is supplied directly into the fluid.

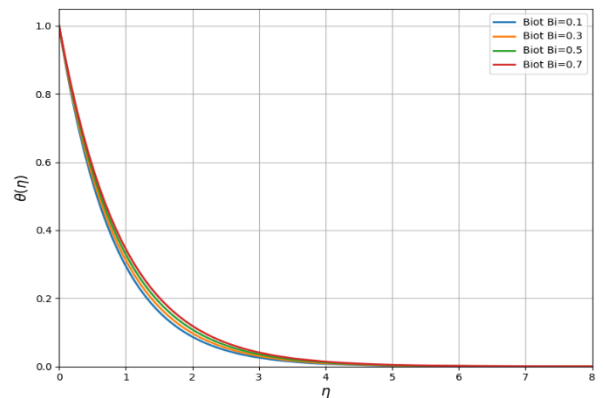


Figure 12: Effects of Biot  $Bi$  on temperature profiles for Blasius flow

Increasing  $Bi$  represents stronger convective cooling at the plate surface, reducing the temperature near the wall. Demonstrates coupled convective heat transfer for finite surface heat exchange.

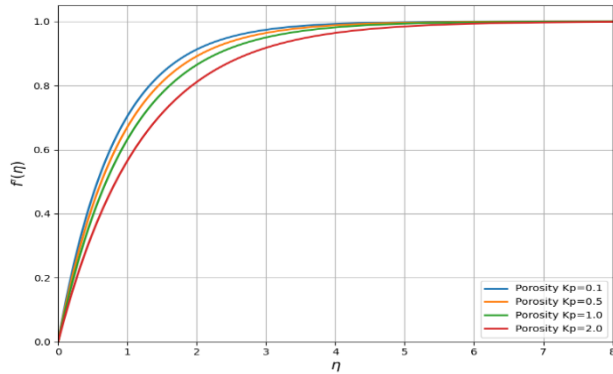


Figure 13: Effects of Porosity  $K_p$  on velocity profiles for Sakiadis flow

Velocity (Figure 13): Higher  $K_p$  slightly reduces the momentum boundary layer due to plate motion dominating the flow.

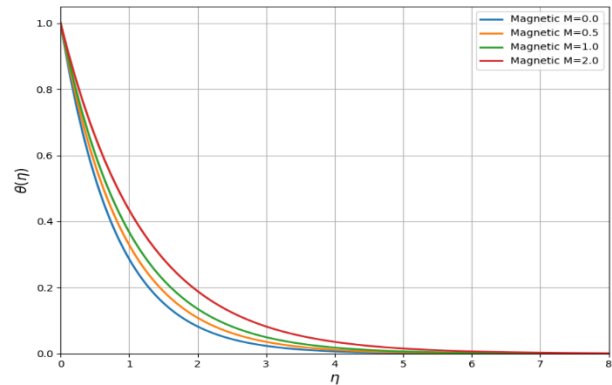


Figure 16: Effects of Magnetic  $M$  on temperature profiles for Sakiadis flow

Slower fluid motion increases temperature along the boundary layer, confirming MHD damping.

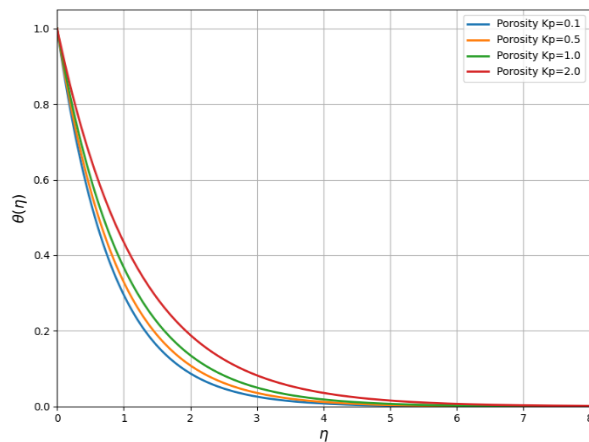


Figure 14: Effects of Porosity  $K_p$  on temperature profiles for Sakiadis flow

Thermal boundary layer thickens as porosity increases, similar to Blasius, but the moving plate enhances near-wall convection.

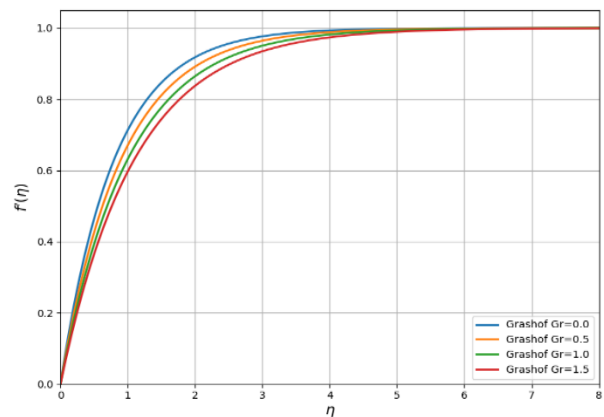


Figure 17: Effects of Grashof  $Gr$  on velocity profiles for Sakiadis flow

Increasing the thermal Grashof number enhances the velocity distribution since buoyancy forces strengthen the flow near the moving plate..

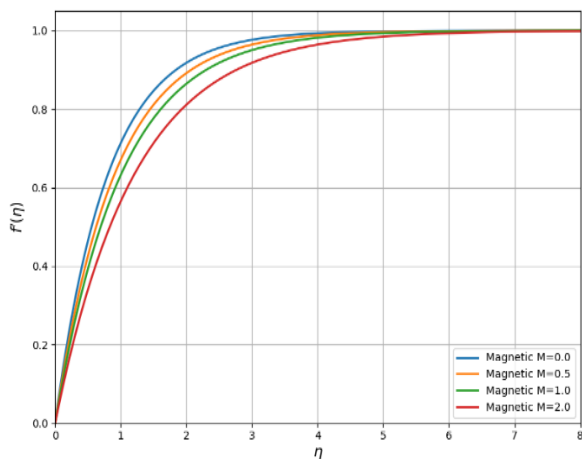


Figure 15: Effects of Magnetic  $M$  on velocity profiles for Sakiadis flow

Lorentz forces oppose the moving plate, reducing velocity near the wall.

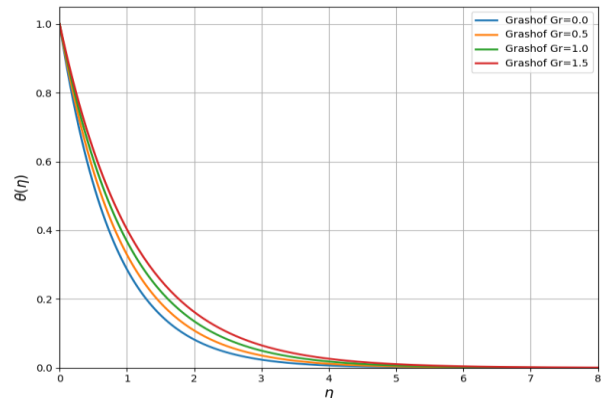


Figure 18: Effects of Grashof  $Gr$  on temperature profiles for Sakiadis flow

As the thermal Grashof number increases, natural convection becomes stronger, which alters the temperature field and enhances heat transport away from the surface.

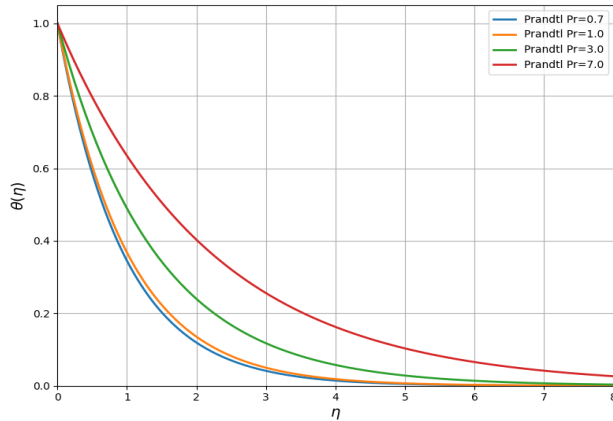


Figure 19: Effects of Prandtl Pr on temperature profiles for Sakiadis flow

Higher Pr fluids (viscous oils) thin the thermal boundary layer, reducing temperature diffusion. Demonstrates the role of fluid properties on heat transfer, central to your study aim.

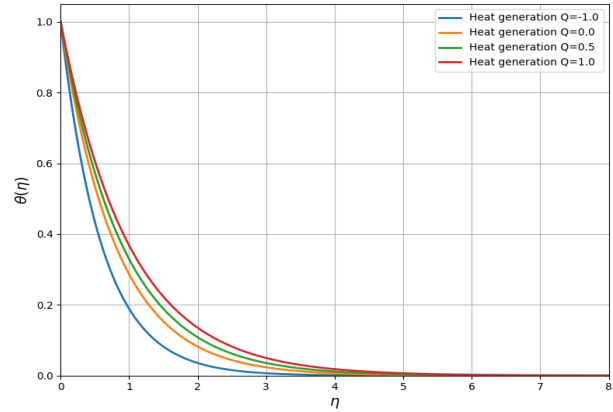


Figure 22: Effects of Heat generation Q on temperature profiles for Sakiadis flow

The temperature distribution increases significantly as the heat generation parameter increases, since heat is continuously supplied into the fluid domain.

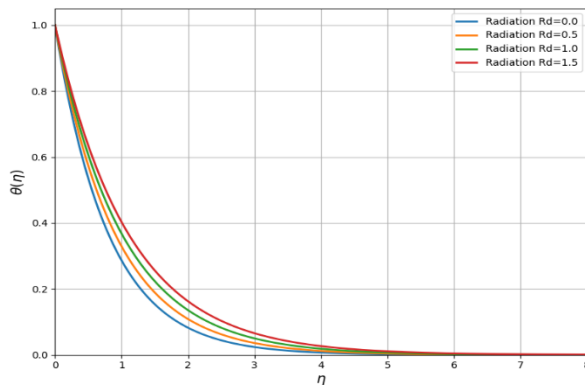


Figure 20: Effects of Radiation Rd on temperature profiles for Sakiadis flow

Radiation increases boundary layer temperatures, similar to Blasius flow, reinforcing thermal radiation importance.

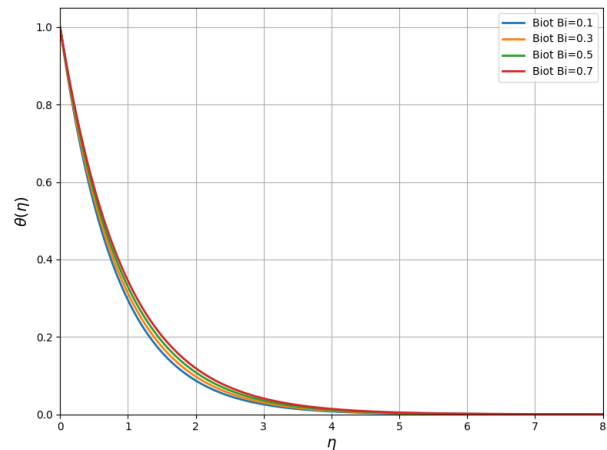


Figure 23: Effects of Biot Bi on temperature profiles for Sakiadis flow

Higher Bi leads to stronger convective cooling at the surface, reducing temperature near the wall. Confirms the effectiveness of surface heat transfer conditions in Sakiadis flow.

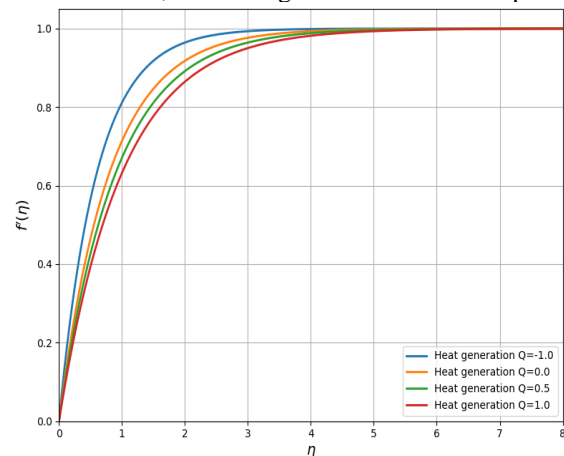


Figure 21: Effects of Heat generation Q on velocity profiles for Sakiadis flow

Increasing the internal heat generation parameter increases the velocity profile due to enhanced buoyancy effects resulting from additional heat energy

Table 1 presents the numerical values of the governing dimensionless parameters used in the computations. These parameters include the magnetic field parameter M, thermal Grashof number Gr, radiation parameter Rd, Prandtl number Pr, internal heat generation parameter Q, porosity parameter K, and Biot number Bi. The selected parameter ranges are consistent with those commonly reported in boundary layer heat transfer studies and represent realistic physical conditions encountered in engineering systems.

The magnetic parameter M controls the strength of the Lorentz force acting on the electrically conducting fluid. The thermal Grashof number Gr characterizes buoyancy effects due to temperature differences between the plate and the surrounding fluid. The Prandtl number Pr represents the ratio of momentum diffusivity to thermal

diffusivity and determines the relative thickness of velocity and thermal boundary layers. The radiation parameter  $R_d$  accounts for thermal radiation effects using the Rosseland approximation, while the heat generation parameter  $Q$  represents volumetric heat sources or sinks within the fluid. The Biot number  $B$  describes the strength of convective heating at the plate surface, and the porosity parameter  $K$  accounts for resistance due to the porous medium.

The chosen parameter values therefore allow a systematic investigation of the combined effects of magnetohydrodynamics, thermal radiation, buoyancy forces, internal heat generation, and convective heating on boundary layer flow and heat transfer over a vertical plate.

Table 2 presents the computed dimensionless velocity and temperature values obtained using the shooting technique combined with the fifth-order Runge–Kutta numerical scheme. The numerical results demonstrate stable convergence of the velocity and temperature profiles for both Blasius and Sakiadis flow configurations.

The shooting technique transforms the boundary value problem into an equivalent initial value problem, allowing the unknown boundary conditions at infinity to be determined iteratively. The fifth-order Runge–Kutta scheme provides high numerical accuracy and stability in solving the coupled nonlinear ordinary differential equations obtained after similarity transformation.

The results confirm that the numerical approach effectively captures the influence of the controlling parameters on both momentum and heat transfer processes. The computed values serve as the basis for generating the graphical results shown in Figures 1–23 and provide quantitative insight into how variations in physical parameters modify the boundary layer structure. Figures 1–12 illustrate the effects of various physical parameters on the velocity and temperature distributions for the classical Blasius flow configuration.

Figures 1 and 2 show the effect of the porosity parameter on the velocity and temperature profiles. Increasing the porosity parameter reduces the velocity within the boundary layer due to the additional resistance introduced by the porous medium. At the same time, the temperature slightly increases because the reduced fluid motion weakens convective heat transport, allowing more heat to accumulate within the boundary layer.

Figures 3 and 4 present the influence of the magnetic field parameter on velocity and temperature profiles. The velocity decreases as the magnetic parameter increases because the Lorentz force generated by the applied magnetic field opposes the motion of the electrically conducting fluid. Consequently, the temperature increases due to reduced convective heat transport, leading to a thicker thermal boundary layer.

Figures 5–7 show the effects of the thermal Grashof number on the velocity and temperature distributions. Increasing the thermal Grashof number enhances the buoyancy force generated by temperature differences, which accelerates the fluid flow and increases the velocity within the boundary layer. The enhanced convection also modifies the temperature field and promotes heat transfer away from the surface.

Figures 8 and 9 illustrate the influence of thermal radiation on the velocity and temperature fields. As the radiation parameter increases, additional thermal energy is introduced into the system, which increases the temperature distribution and slightly enhances the fluid velocity due to increased buoyancy effects.

Figures 10 and 11 demonstrate the impact of internal heat generation on the velocity and temperature profiles. Increasing the heat generation parameter introduces additional thermal energy into the fluid, resulting in higher temperatures and a slight increase in velocity due to stronger buoyancy-driven flow.

Figure 12 shows the effect of the Biot number on the temperature profile. Increasing the Biot number represents stronger convective heating at the plate surface, which increases the temperature distribution within the boundary layer.

Figures 13–23 illustrate the behavior of the velocity and temperature fields for the Sakiadis flow configuration, where the plate moves relative to the fluid.

Figures 13 and 14 show that increasing the porosity parameter reduces the velocity while increasing the temperature profile. This behavior is similar to the Blasius case and occurs due to the resistance imposed by the porous medium.

Figures 15 and 16 show that the magnetic field parameter significantly suppresses the velocity due to the Lorentz force acting opposite to the fluid motion. The reduction in velocity leads to increased temperature within the boundary layer due to decreased convective heat transport.

Figures 17 and 18 demonstrate that increasing the thermal Grashof number enhances the velocity distribution due to stronger buoyancy forces while modifying the temperature field through enhanced natural convection.

Figure 19 shows the influence of the Prandtl number on the temperature profile. Higher Prandtl numbers reduce the thermal boundary layer thickness because fluids with large Prandtl numbers possess lower thermal diffusivity.

Figure 20 illustrates the effect of thermal radiation on the temperature distribution. Increasing the radiation parameter increases the temperature within the boundary layer due to enhanced radiative heat transfer.

Figures 21 and 22 demonstrate the effects of internal heat generation on velocity and temperature profiles. The presence of internal heat sources increases the fluid temperature and enhances buoyancy-driven motion.

Finally, Figure 23 shows the effect of the Biot number on the temperature distribution. An increase in the Biot number strengthens convective heat transfer at the surface, leading to higher temperatures near the plate.

Therefore, the numerical results presented in Tables 1 and 2 and Figures 1–23 clearly demonstrate how magnetohydrodynamic effects, thermal radiation, buoyancy forces, internal heat generation, and convective heating influence the velocity and temperature fields in boundary layer flows over a vertical plate. The results also highlight the differences between the Blasius and Sakiadis flow configurations under identical physical conditions.

These findings provide important physical insight into the behavior of MHD boundary layer flows and contribute to improved understanding of heat transfer mechanisms in engineering systems involving electrically conducting fluids.

## CONCLUSION

This study investigated the steady two-dimensional magnetohydrodynamic boundary-layer flow with heat transfer characteristics of an incompressible fluid flowing over a vertical plate for both Blasius (stationary surface) and Sakiadis (moving surface) flow configurations. The effects of key physical parameters including porosity, magnetic field, thermal buoyancy, thermal radiation, internal heat generation, Biot number, and Prandtl number. *The transformed similarity equations were solved numerically using the shooting method coupled with a fifth-order Runge–Kutta integration technique.*

The numerical results show that increasing the porosity parameter enhances fluid penetration and thermal diffusion in both flow regimes. Increasing the magnetic parameter significantly suppresses the motion of the electrically conducting fluid due to Lorentz forces, leading to reduced velocity profiles and increased temperature distributions. Buoyancy forces, represented by the thermal Grashof number, enhance natural convection and strongly influence both velocity and temperature fields. Thermal radiation primarily affects the energy transport, resulting in thicker thermal boundary layers, while its influence on velocity is relatively weak. Internal heat generation raises the fluid temperature and slightly accelerates the flow, whereas heat absorption produces the opposite effect. The Biot number controls surface convective heat transfer, with higher values leading to lower wall temperatures. Additionally, increasing the Prandtl number leads to a thinner thermal boundary layer because of lower thermal diffusivity.

This analysis demonstrates the combined effects of magnetohydrodynamic forces, buoyancy effects, thermal radiation, porous medium resistance, and convective heating on the velocity and temperature distributions in both Blasius and Sakiadis flows. The findings are relevant to engineering applications including thermal management of electronic components, thermal insulation technologies, geothermal energy, and *magnetohydrodynamic flow control applications*. The model can be extended to unsteady flows, non-Newtonian fluids, or inclined plates for future investigations.

## REFERENCE

- Ahmed, S., & Musa, A. (2022). Numerical investigation of heat transfer in magnetohydrodynamic boundary layer flow over a vertical surface. *Journal of Basic and Applied Scientific Research*, 14(1), 45–56.
- Anderson, J.D. (1995). *Computational fluid dynamics: The basics with applications*. McGraw-Hill, New York
- Bataller, R. C. (2008). Radiation effects in the Blasius flow. *Applied Mathematics and Computation*, **198**, 333–338.
- Bejan, A. (2013). *Convection Heat Transfer* (4th ed.). John Wiley and sons, New York.
- Blasius, H. (1908). Boundary layers in fluids with little friction. *Z. Math. Phys.*, **56**, 1–37.
- Chamkha, A.J. (2001). Hydromagnetic flow and heat transfer over continuous moving surface with heat generation or absorption. *International journal of Engineering Science*, 39, 1181-1198
- Incropera, F. P., DeWitt, D. P., Bergman, T. L., & Lavine, A. S. (2011). *Fundamentals of Heat and Mass Transfer* (7th ed.). Wiley.
- Mahapatra, T.R. and Gupta, A.S. (2002). Heat transfer in stagnation-point flow towards a stretching sheet. *Heat and Mass transfer* 38, 517-521
- Sakiadis, B.C. (1961). Boundary layer behavior on continuous solid surface: I. Boundary-layer equations for two-dimensional and axisymmetric flow. *AIChE Journal*, 7, 26-28